

# Dendrimer-based Hydrogels with Controlled Drug Delivery Property for Tissue Adhesion

Ya-Qiang Wang<sup>a,b</sup>, Xue-Yu Dou<sup>a,b</sup>, Hu-Fei Wang<sup>a,b</sup>, Xing Wang<sup>a,b\*</sup>, and De-Cheng Wu<sup>a,c\*</sup><sup>a</sup> Beijing National Laboratory for Molecular Sciences, State Key Laboratory of Polymer Physics & Chemistry, Institute of Chemistry, Chinese Academy of Sciences, Beijing 100190, China<sup>b</sup> University of Chinese Academy of Sciences, Beijing 100049, China<sup>c</sup> Department of Biomedical Engineering, Southern University of Science and Technology, Shenzhen 518055, China

**Abstract** In recent years, the hydrogel-based tissue adhesives have been extensively investigated for their excellent biocompatibility and the ability to be administered directly within the adherent tissue. To meet the requirement for more controllable release in various physiological settings, the components of hydrogel adhesive should be more precisely tailored. In this work, the POSS-ace-PEG hydrogel adhesive was fabricated with the polyacetal dendrimer G1'-[NH<sub>3</sub>Cl]<sub>16</sub> and poly(ethylene glycol) succinimidyl carbonate (PEG-SC) due to the regular peripheral amino structure of G1'-[NH<sub>3</sub>Cl]<sub>16</sub>. Rheological and adhesion tests demonstrated that the hydrogel adhesive had good mechanical and adhesive properties, which could effectively adhere to the pigskin and severed nerves. Moreover, the tissue adhesive exhibited good stability under neutral conditions and the rapid degradation under acidic conditions, allowing for the release of doxycycline hydrochloride (DOX) drug in response to pH. Together, these results suggested that the POSS-ace-PEG adhesive had the potential to provide an alternative to tissue adhesives for applications in pathological environments (inflammation, tumors, etc.).

**Keywords** Hydrogel adhesive; Dendrimer; pH-Responsive; Drug delivery; Tissue adhesion

**Citation:** Wang, Y. Q.; Dou, X. Y.; Wang, H. F.; Wang, X.; Wu, D. C. Dendrimer-based hydrogels with controlled drug delivery property for tissue adhesion. *Chinese J. Polym. Sci.* 2021, 39, 1421–1430.

## INTRODUCTION

Tissue adhesives are a kind of materials that adhere to tissue and bond different tissues (e.g., skins, muscles and nerve tissues) together to achieve proper healing and prevent gas or fluid leakage from the tissue.<sup>[1–3]</sup> They are essentially non-invasive and can be utilized conveniently without special requirements.<sup>[4]</sup> Hydrogels are 3D cross-linked networks of polymeric matrices that can absorb a large amount of water or biological fluids in their swollen state thanks to the presence of hydrophilic groups (such as hydroxyl, amino or carboxyl groups) within their backbones. Due to the high water absorption properties of hydrogels, they can mimic the properties of biological tissues with the excellent biocompatibility.<sup>[5,6]</sup> Unlike conventional adhesives, hydrogel-based adhesive materials can effectively penetrate oxygen to the wound surface and cool the wound site,<sup>[7,8]</sup> thereby reducing patient pain. Besides, hydrogel adhesives have the property of encapsulating drug molecules and growth factors *in situ* and releasing them directly at the bonded surface, reducing loss in the humoral environment.<sup>[9]</sup> Especially for controlled delivery, drug-loaded hydrogels need to release them in a controlled manner with adjustable stability

and biodegradability.<sup>[10,11]</sup> Therefore, it is necessary to develop *in situ* hydrogel adhesives with biocompatibility and controlled drug release capability.

Over the years, there is a great demand for stimulus-responsive hydrogels in the medical field on account of their unique properties.<sup>[12–14]</sup> Several hydrogels have been reported to be responsive to pH, temperature and light.<sup>[15–17]</sup> Among them, pH-responsive hydrogel systems have been widely researched for controlled drug delivery of various therapeutic agents, ranging from chemotherapeutic agents to small molecule drugs and proteins.<sup>[18–21]</sup> Changes *in vivo* pH can occur in intracellular lysosomes, cancerous or inflamed tissues, or organs such as the vagina or gastro/intestinal tract.<sup>[22]</sup> When the therapeutic molecules are dissolved or encapsulated or electrostatically bound to hydrogel networks, it is the change in surrounding pH that triggers the controlled release of these drug-loaded hydrogels.<sup>[23,24]</sup> This pH response can be tailored by careful fabrication of the monomeric components to be delivered in a specific physiological condition.<sup>[25]</sup> In particular, some pathological environments like cancer<sup>[18]</sup> or inflammatory<sup>[26]</sup> are slightly acidic; therefore, chemical groups with acid cleavable, such as acetals,<sup>[27]</sup> ketals,<sup>[28]</sup> tertiary esters,<sup>[29]</sup> imines,<sup>[30]</sup> ortho esters,<sup>[31]</sup> hydrazones<sup>[32]</sup> are increasingly being introduced into the structure of acid-responsive hydrogels. Among them, acetal bonds are of great interest because of their pH sensitivity and non-acidic metabolites.<sup>[33]</sup> Our group previously

\* Corresponding authors, E-mail: wangxing@iccas.ac.cn (X.W.)

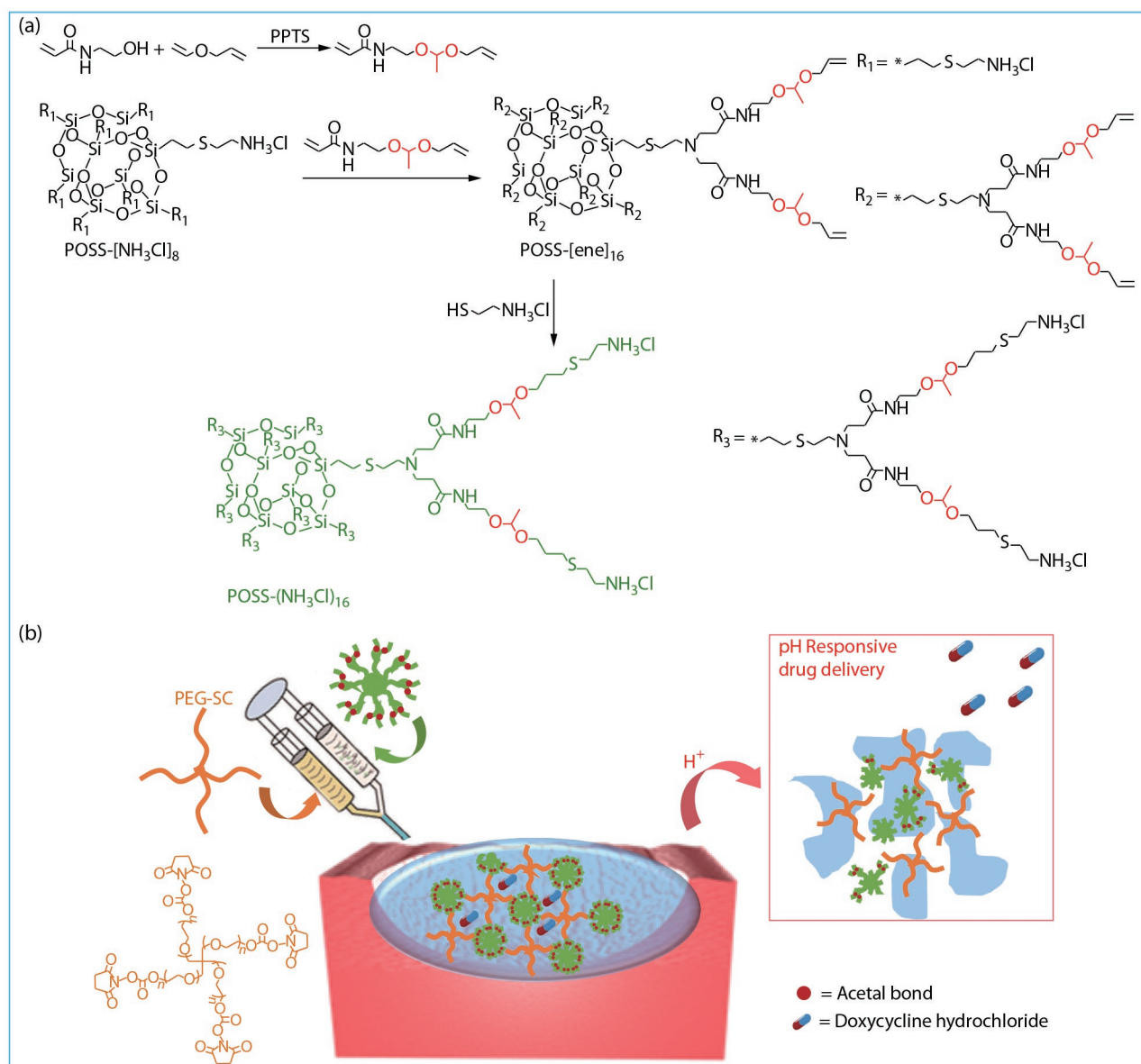
E-mail: wudc@sustech.edu.cn (D.C.W.)

Received March 22, 2021; Accepted March 30, 2021; Published online May 28, 2021

focused on acetal bonds to prepare a variety of drug delivery systems, which exhibited satisfactory pH-responsive release effects.<sup>[34–37]</sup> The dendritic polyacetals amid them are of great advantage in the construction of acid-responsive hydrogels.<sup>[35]</sup> Dendrimers are highly branched and regularly structured macromolecules consisting of a core, branching segments (*i.e.*, generation, Gn), and a defined number of peripheral groups.<sup>[38,39]</sup> These polymers offer advantages over linear polymers in terms of size, structure, density and control of functional end groups, and can be easily tailored for specific applications.<sup>[40–42]</sup> In addition, dendritic polymers have regular and numerous functional groups at their ends, allowing an increase in the crosslink density of the hydrogel without significantly increasing polymer concentration.<sup>[43,44]</sup> Therefore, we believe that the use of dendritic polyacetals is a feasible direction for the construction of acid-responsive hydrogel

binders.

Herein, we selected octaammonium polyhedral oligomeric silsesquioxanes (POSS- $[\text{NH}_3\text{Cl}]_8$ ) as a large hydrophobic core to fabricate polyacetal dendrimer G1'- $[\text{NH}_3\text{Cl}]_{16}$ . Benefiting from the regular amino structure of the outer end of G1'- $[\text{NH}_3\text{Cl}]_{16}$ , high molecular weight and multi-armed poly(ethylene glycol) succinimidyl carbonate (PEG-SC) could be cross-linked to construct a kind of hydrogel adhesive, POSS-ace-PEG hydrogel (Scheme 1). This hydrogel adhesive had good mechanical strength and effective adhesion, which could effectively bond with the pigskin and broken nerves. More importantly, due to the presence of acetal, the hydrogel could remain stable under neutral conditions and rapidly degrade in acidic conditions, which enabled pH-responsive release of antibacterial drugs and provided a new idea for the construction of smart tissue adhesive platforms.



**Scheme 1** Synthetic approach of (a) polyacetal dendrimers and (b) fabrication of POSS-ace-PEG hydrogel for tissue adhesion and controlled drug delivery.

## EXPERIMENTAL

### Materials

4-Armed and 8-armed poly(ethylene glycol) succinimidyl carbonate (4-arm PEG-SC,  $M_w=10$  kDa, 20 kDa; 8-arm PEG-SC,  $M_w=20$  kDa,  $M_w/M_n=1.03$ ) were purchased from SINOPEG, China. Octaammonium polyhedral oligomeric silsesquioxane (POSS-[NH<sub>3</sub>Cl]<sub>8</sub>) was synthesized according to the methods given in our previous literature.<sup>[45]</sup> Allyl vinyl ether (95%, Alfa Aesar), *N*-(2-hydroxyethyl) acrylamide (98%, TCI), cysteamine hydrochloride (99%, Energy Chemical), 2,2-dimethoxy-2-phenylacetophenone (DMPA, 99%, J&K), pyridinium 4-toluenesulfonate (PPTS, 99%, Energy Chemical) and doxycycline hydrochloride (DOX, 98%, J&K) were used as received. Tetrahydrofuran (THF), methanol (MeOH), dichloromethane (DCM) and triethylamine (TEA) (reagent grade, Beijing Chemical Works) were purified by stirring over calcium hydride for 24 h followed by distillation. Other solvents and compounds were purchased from Beijing Chemical Works and used without further purification.

### The NMR and MALDI-TOF MS Measurement

Nuclear magnetic resonance (NMR) spectra were recorded on a Bruker 400 MHz spectrometer. Matrix-assisted laser desorption ionization-time of flight mass spectrometry (MALDI-TOF MS) measurements were carried out by using a Bruker BIFLEX III equipped with a 337 nm nitrogen laser.

### Synthesis of Polyacetal Dendrimers

#### Synthesis of *N*-(2-(1-(allyloxy)ethoxy)ethyl)acrylamide (AEEAA)

*N*-(2-hydroxyethyl) acrylamide (6.9 g, 60 mmol) and PPTS (0.125 g, 5 mmol) were dissolved in 50 mL of dry DCM at 0 °C under nitrogen by dropwise addition of allyl vinyl ether (4.2 g, 5 mmol) in 10 mL of dry DCM. The mixture was stirred at room temperature overnight, and then K<sub>2</sub>CO<sub>3</sub> was added to quench the reaction. The mixture was filtered by a pad of celite, after that the filtrate was evaporated under reduced pressure to obtain crude product, which was purified by silica gel chromatography using DCM/ethyl acetate (*V/V*=15/1) containing 1% (*V/V*) TEA as eluent to obtain the acetal monomer AEEAA as a pale-yellow liquid with 70% yield.

#### Synthesis of G1-[ene]<sub>16</sub>

POSS-[NH<sub>3</sub>Cl]<sub>8</sub> (308 mg, 0.2 mmol), AEEAA (1.27 g, 6.4 mmol) and TEA (242 mg, 2.4 mmol) were dissolved in methanol/water (*V/V*=7/3) under stirring at 70 °C for 48 h. The mixture was diluted by DCM followed by washing three times with brine. The organic layer was dried with MgSO<sub>4</sub> and concentrated to a few milliliters, which was then precipitated in diethyl ether/hexane (*V/V*=1/2) for three times. The precipitate was dried under vacuum to give the product G1-[ene]<sub>16</sub> as a viscous yellow oil with 80% yield.

#### Synthesis of G1'-[NH<sub>3</sub>Cl]<sub>16</sub>

G1-[ene]<sub>16</sub> (355 mg, 0.08 mmol), cysteamine hydrochloride (872 mg, 7.68 mmol), and DMPA (97 mg, 0.38 mmol) were dissolved in methanol. The mixture was purged with argon for 10 min and then irradiated under a 365 nm UV lamp at room temperature for 3 h. The crude product was precipitated in diethyl ether twice. The precipitate was dissolved in deionized water and then precipitated in MeOH/THF (*V/V*=1/4) for three

times. Finally, the yellow oiled precipitate was dried under vacuum to give the product G1'-[NH<sub>3</sub>Cl]<sub>16</sub> as a pale-yellow solid with 50% yield.

### Preparation of Hydrogels

Firstly, precursor solution **1** was prepared by dissolving dendritic polyacetal G1'-[NH<sub>3</sub>Cl]<sub>16</sub> in 0.05 mol/L Na<sub>2</sub>CO<sub>3</sub> solution, while a different kind of precursor solution **2** were prepared by dissolving multi-arm and multi-molecular weight PEG-SC in the phosphate buffer (pH 7.4) with the same solid content (12%) of PEG-SC (4-armed PEG-SC,  $M_w=10$  kDa, 20 kDa, 40 kDa; 8-armed PEG-SC,  $M_w=20$  kDa). All the operations were performed at room temperature. Finally, the same volume of precursor solutions **1** and **2** were simultaneously injected into the molds to obtain POSS-ace-PEG hydrogels using a dual syringe.

### Measurement of Gelation Time

The gelation time was determined by the vial tilting method. We prepared the hydrogels in sample vials. The solution was mixed and the vials were inverted until the solution could no longer flow. The time at which this phenomenon happened was designated as the gelation time.

### Rheological Studies

Rheometry test was performed on a Thermo Haake with a plate geometry (diameter=35 mm) at 25 °C. The hydrogel discs (diameter=35 mm, thickness=1.2 mm) were tested at a gap distance of 1 mm. Before the tests, an amplitude sweep was first performed in order to define the linear viscoelastic region (LVR) in which the storage modulus is independent to the strain amplitude. Then an angular frequency  $\omega$  of 10 rad/s and a deformation amplitude  $\gamma_0$  of 0.1% were selected to perform the rheological studies.

### Scanning Electron Microscopy (SEM)

Several kinds of POSS-ace-PEG hydrogels were prepared according to the method described above and then freeze-dried at 50 °C for 24 h. Then the dried samples were carefully stuck onto the conducting resin with double-sided adhesive and were sputter-coated with a thin layer of Pt for 120 s to make the sample conductive before testing. Field emission scanning electron microscopy (FESEM) images were obtained at an acceleration voltage of 5 kV on a JSM-6700F microscope (JEOL, Japan).

### Measurement of Adhesion Strength

The adhesion tests were conducted using a universal tensile machine (3365 Instron, USA) with a force sensor of 100 N by the standard lap-shear test (ASTM F2255). All tests were conducted with a constant tensile speed of 10 mm/min. Briefly, adhered samples with an adhesion area of 2.5 cm (width) × 1 cm (length) were prepared and the other sides were stuck on the machine at ambient temperature. When the attaching porcine skins were torn apart under the driven force, the shear strength was measured and examined with three parallel groups. Shear strength was determined by dividing the maximum force by the adhesion area.<sup>[46]</sup>

### Swelling and Degradation Profiles

The POSS-ace-PEG hydrogels were immersed in PBS and incubated at 37 °C to evaluate their swelling behavior. To calculate the swelling ratio, the wet weight of the swollen hydrogel at each time point ( $W_t$ ) was normalized to the weight of the unswollen hydrogel at the beginning, referred to as the

initial weight of the hydrogel ( $W_i$ ) right after gelation, using the following equation:

$$\text{Swelling ratio(\%)} = W_s/W_i \times 100\% \quad (1)$$

For acidic degradation test, fully swollen POSS-ace-PEG hydrogels were treated with pH=5.0 buffer solution. The weight of the remaining hydrogel was measured at each time point as mentioned before. In the swelling and degradation experiments, the pristine PEG hydrogels made of 4-armed PEG-SC ( $M_w=20$  kDa) and 4-armed PEG-NH<sub>2</sub> ( $M_w=20$  kDa) with the same solid content are chosen to be the control groups.

### Drug Loading and Drug Release

Doxycycline hydrochloride (DOX) was used as the model drug to investigate drug release properties of POSS-ace-PEG hydrogels in different pH conditions. Briefly, 0.4 mg of DOX was dissolved in 400  $\mu$ L of PEG-SC solution. Then, the solution was mixed with 400  $\mu$ L of G1'-[NH<sub>3</sub>Cl]<sub>16</sub> solution to obtain DOX-loaded POSS-ace-PEG hydrogel. The DOX concentration in the hydrogels was fixed at 0.5 mg/mL. The obtained hydrogels were incubated in 5 mL of PBS (pH=7.4 and 5.0) solution at 37 °C with 100 r/min of constant stirring. At each interval time point, all volumes of released medium were taken out for UV-Vis analysis and then 5 mL of fresh solution was added. The concentrations of DOX were analyzed by a spectrophotometer (Lambda 950, PerkinElmer, UK) at a wavelength of 350 nm. The cumulative amount of the drug was calculated by the following equation:

$$R_i = \frac{\sum_1^i V_j C_j}{m_{\text{drug}}} \times 100\% \quad (i \geq 1) \quad (2)$$

where  $V_j$  is the extraction sample volume, and  $C_j$  is the concentration of DOX in the extraction sample. All measurements were conducted in triplicate.

### Cytotoxicity Studies

The cell viability of the hydrogels and the degradation products were studied by quantitative CCK-8 cytotoxicity assay. The 3T3 mouse fibroblasts (the China Infrastructure of Cell Line Resource) were suspended in cell culture medium and seeded into 96-well microculture plates with a density of  $1 \times 10^4$  cells/100 $\mu$ L in each well and incubated at 37 °C for 24 h in a 5% CO<sub>2</sub> humidified incubator to obtain a monolayer of cells. Several kinds of gels (1.0 g) were immersed in the fresh cell medium (10 mL) for 24 h to get the extracts. Then, the treated cell medium was used to replace fresh cell medium and the cells were further incubated for an additional time (1 and 3 days). The cells cultured in fresh medium were used as control. At the preset time, the sample solution was removed and fresh medium was added with 10  $\mu$ L of acetone containing CCK8 (1 mg/mL) for 2 h. Finally, the absorbance of the sample solution was detected at 620 nm (reference 450 nm). The relative cell viability was calculated as the ratio between the mean absorbance value of the sample and that of the control group. Samples with relative cell viability less than 70% were deemed to be cytotoxic. Seven independent cultures were prepared and cytotoxicity test was repeated three times for each culture. For the cytotoxicity of the degradation products, gels (1.0 g) were immersed in the fresh cell medium (10 mL) until complete degradation. Then the cell medium containing the degradation products was used to incubate the cells, following the procedure used before.

### Pigskin and Nerve Adhesion

To evaluate the adhesion of the POSS-ace-PEG hydrogels, we investigated their adherence to pigskin. Pigskin was selected due to its biological similarity to human dermis. The hydrogels were mixed with a small amount of rhodamine B and formed *in situ* on the surface of the skin by using a dual syringe. Then torsion stress was applied to the hydrogels to test their adherence flexibility on the skin. Also, we used adhesive POSS-ace-PEG hydrogels to splice the broken sciatic nerves which are proximal of the bifurcation at the knee and distal from the spinal column. Firstly, the sciatic nerve explants were taken from the legs of Sprague-Dawley rat (Beijing Vital River Laboratory Animal Technology Co., Ltd.) by the surgical scissors. We clipped the sciatic nerve into two pieces. Then, two pieces of broken sciatic nerves were got closer and aligned with each other by the forceps. The POSS-ace-PEG hydrogel precursors were applied on the joint of the two broken pieces, holding them together for 1 min to make sure that the hydrogel was formed completely.

## RESULTS AND DISCUSSION

### Synthesis of G1'-[NH<sub>3</sub>Cl]<sub>16</sub> Polyacetal Dendrimer

Based on the previous experience of our group,<sup>[37]</sup> we synthesized a kind of dendritic polyacetal with 16 amino groups at the end. The specific route was shown in Scheme 1(a). Firstly, we synthesized the asymmetric acetal monomer (AEEAA) with an allyl group at one end and acrylamide at the other end through acetal reaction (Fig. 1A). Then, we chose octaamine hydrochloride POSS (POSS-[NH<sub>3</sub>Cl]<sub>8</sub>) as the core to synthesize dendritic polyacetal. POSS has good stability as a cubic cage molecule composed of inorganic substances, whose eight amino hydrochlorides on the periphery are evenly distributed on its eight vertices,<sup>[47–50]</sup> which cannot be affected by space hindrance to influence the efficiency of the reaction.<sup>[45,51]</sup> On this basis, we constructed G1-[ene]<sub>16</sub> dendritic polyacetal through Michael addition reaction. In the <sup>1</sup>H-NMR spectrum of G1-[ene]<sub>16</sub> (Fig. 1B), the formation of a double bond peak at  $\delta=5.0$ –6.0 ppm proved the successful synthesis of G1-[ene]<sub>16</sub> product. The MALDI-TOF MS spectrum of G1-[ene]<sub>16</sub> is shown in Fig. 1(D), although the ionization of silicon-containing compounds is difficult, the peak shape of the obtained spectrum is a little messy,<sup>[52]</sup> while the peak position  $m/z$  is about 4437, which was corresponding to the calculated value of 4438 of the G1 generation product. Finally, we constructed the final product G1'-[NH<sub>3</sub>Cl]<sub>16</sub> through the "thiol-ene" reaction under UV light. From the <sup>1</sup>H-NMR spectrum of G1'-[NH<sub>3</sub>Cl]<sub>16</sub> (Fig. 1C), the disappearance of the double bond peak at  $\delta=5.0$ –6.0 ppm proved the normal progression of the "thiol-ene" reaction. The ratio of characteristic peaks at  $\delta=4.7$  and 1.3 ppm (i, j) was kept at 1:3, which proved the stability of the acetal structure in G1'-[NH<sub>3</sub>Cl]<sub>16</sub>. Since the end of G1'-[NH<sub>3</sub>Cl]<sub>16</sub> contained many amino groups, it could not be characterized by MALDI-TOF MS and GPC, but the integral ratio of characteristic peaks in the <sup>1</sup>H-NMR spectrum was consistent with the expectations, proving the successful preparation of G1'-[NH<sub>3</sub>Cl]<sub>16</sub>.

### Preparation of the POSS-ace-PEG Hydrogels

Since the periphery of G1'-[NH<sub>3</sub>Cl]<sub>16</sub> was uniformly distributed with 16 amino groups, it could form a cross-linked network by

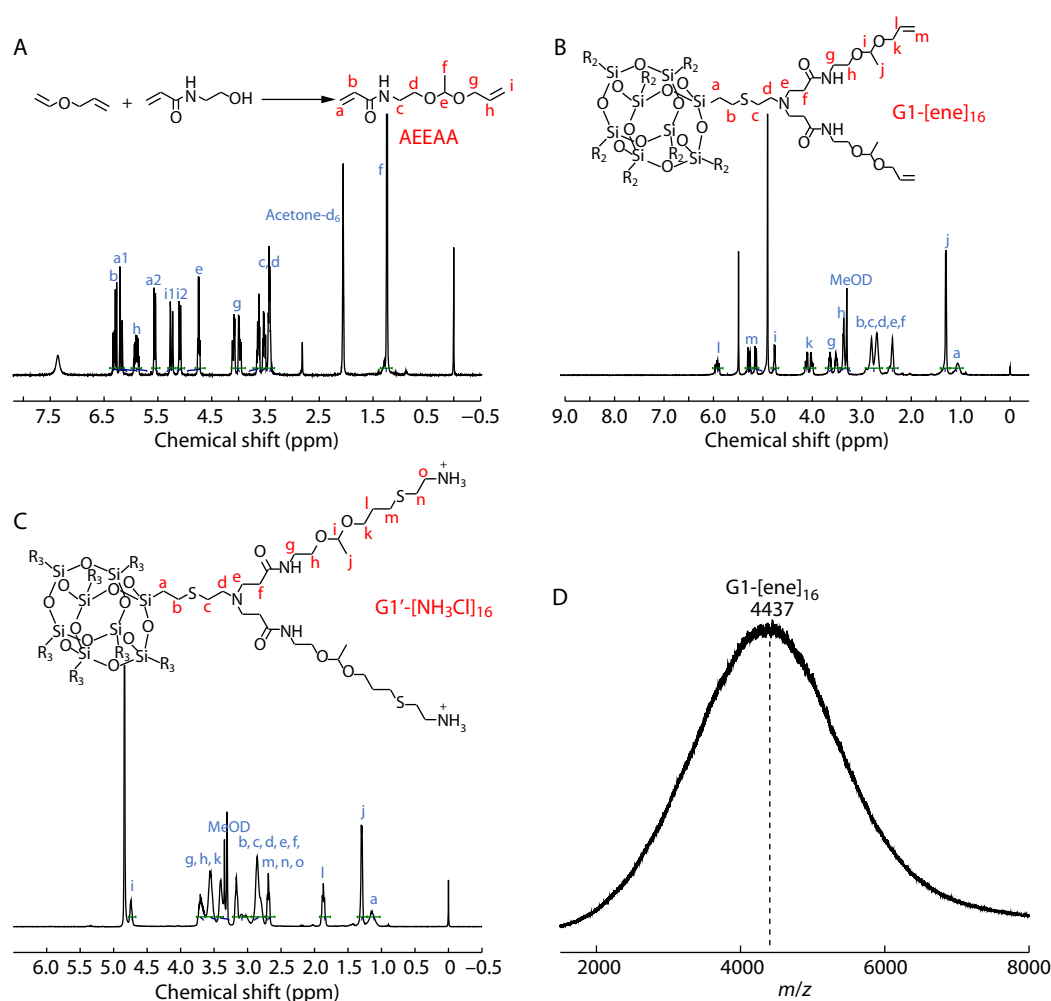


**Fig. 1**  $^1\text{H-NMR}$  spectra of (A) AEEAA, (B)  $\text{G1}^-[\text{NH}_3\text{Cl}]_{16}$  and (C)  $\text{G1}'-[\text{NH}_3\text{Cl}]_{16}$ ; (D) MALDI-TOF MS spectrum of  $\text{G1}^-[\text{ene}]_{16}$ .

amidation reaction with structurally regular multi-armed poly(ethylene glycol) succinimide carbonate (PEG-SC). Firstly,  $\text{G1}'-[\text{NH}_3\text{Cl}]_{16}$  needed to be deprotonated by dissolving in alkaline solution to enable the amino groups to undergo the amidation reaction completely. We used a two-channel syringe method to dissolve each ingredient in solution and extrude them together to form POSS-ace-PEG hydrogels, which was easy to handle even for some critical medical needs requiring rapid bonding. We fixed the solid content of PEG at 6% and investigated the effect of different types of PEG-SC with different ratios of reactive functional groups on gelation time. As shown in Fig. 2, gelation time of PEG-SC with 4-arm 10 k, 4-arm 20 k and 8-arm 20 k co-blended with  $\text{G1}'-[\text{NH}_3\text{Cl}]_{16}$  (POSS-tetra-PEG<sub>10k</sub>, POSS-tetra-PEG<sub>20k</sub> and POSS-octa-PEG<sub>20k</sub>) exhibited similar trends: when the ratio of amino groups of  $\text{G1}'-[\text{NH}_3\text{Cl}]_{16}$  to succinimidyl ester groups of PEG-SC ( $\text{NH}_2:\text{NHS}$ ) was between 1.5 and 1, the gelation time was all in the range of 10–20 s, showing a fast gelation rate; when the ratio of  $\text{NH}_2:\text{NHS}$  was lower than 1, the gelation rate became significantly slower with the decrease of  $\text{NH}_2$  content. In this system, effective crosslinking of PEG molecules in the blend system was a necessary factor for the formation of gelation transition.  $\text{G1}'-[\text{NH}_2]_{16}$  had a lower molecular weight and a large number of

functional groups; while PEG-SC had a small number of functional groups but a high molecular weight. Therefore, when the ratio of  $\text{NH}_2:\text{NHS}$  is slightly greater than 1, PEG molecules could achieve complete cross-linking, thus leading to rapid gelation; when the ratio of  $\text{NH}_2:\text{NHS}$  was slightly less than 1, succinimidyl ester groups cannot completely react and the cross-linking of PEG molecules was weakened, so the gelation transition became slower. Because the gelation time was nearly equivalent when  $\text{NH}_2:\text{NHS}=1-1.5$ , we used the ratio of  $\text{NH}_2:\text{NHS}=1$  to prepare all hydrogels in the subsequent experiments out of consideration for saving polyacetal dendrimers.

### Viscoelasticity of the POSS-ace-PEG Hydrogels

The viscoelasticity of different types of POSS-ace-PEG hydrogels was tested under deformation oscillation measurements to examine the stability of hydrogels. The  $G'$  values of all hydrogel groups were greater than the  $G''$  values, which indicated that the three groups of hydrogels could maintain a stable gel state over a long time. Also, the  $G'$  values showed the following trend: POSS-tetra-PEG<sub>10k</sub>>POSS-tetra-PEG<sub>20k</sub>>POSS-octa-PEG<sub>20k</sub> (Fig. 3). The superior storage modulus of POSS-tetra-PEG<sub>10k</sub> hydrogel was ascribed to its high density of cross-linking points. At the same time, the homogeneity of gel network was also an

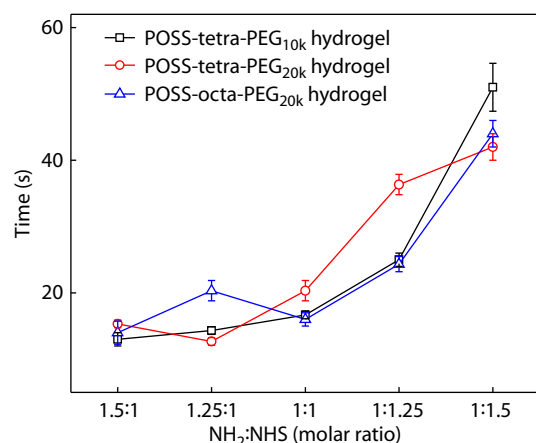


**Fig. 2** Gelation time of various POSS-ace-PEG hydrogels.

important factor in affecting the storage modulus. 8-Arm PEG-SC with more arms retained residual unreacted functional groups during the gel formation, and thus the homogeneity of the network was poor, resulting in the lower  $G'$  value of the POSS-octa-PEG<sub>20k</sub> hydrogel. Overall, all the three groups of hydrogels maintained stable for a long time, which was favorable to be used in practical applications.

### Morphologies of the POSS-ace-PEG Hydrogels

SEM was used to observe the microstructure of POSS-ace-PEG hydrogels. All lyophilized POSS-ace-PEG hydrogels show 3D interconnected pore structures despite variation in the pore size (Fig. 4). The POSS-tetra-PEG<sub>10k</sub> hydrogel shows a denser network structure with small and dense cavities; while the POSS-tetra-PEG<sub>20k</sub> hydrogel network has a sparser distribution of pores and larger pore sizes. In contrast, POSS-octa-PEG<sub>20k</sub> hydrogel network appears to be more disorganized with uneven pore size. These microscopic morphology pictures were also consistent with rheological results of the hydrogels. POSS-tetra-PEG<sub>10k</sub> hydrogel had a more compact network structure with the highest storage modulus; while the POSS-octa-PEG<sub>20k</sub> hydrogel had the lowest  $G'$  value due to the worst homogeneity of its network.

### Adhesion Strength of POSS-ace-PEG Hydrogels

The succinimidyl ester groups in POSS-ace-PEG hydrogels could chemically bind with  $-NH_2$  and  $-SH$  on the surface of human tissues,<sup>[43]</sup> playing a role in tissue adhesion during the *in situ* gelation process. Since the biological properties of porcine skin are similar to those of human dermis, we chose porcine skin as the tissue model for adhesion measurement. We applied the POSS-ace-PEG hydrogel *in situ* between two pig skins and measured the shear strength between the pig skins after the gel was cured, which could show the maximum force within the adhesion area. From the Fig. 5, we could observe the trend of shear strength: POSS-tetra-PEG<sub>20k</sub> > POSS-tetra-PEG<sub>10k</sub> > POSS-octa-PEG<sub>20k</sub>. For adhesives, the adhesion energy of the material comes partly from the interfacial energy between the material and the adhesion interface, and partly from the intrinsic strength of the adhesive after curing.<sup>[46]</sup> According to the rheological results, the modulus order of gels was: POSS-tetra-PEG<sub>10k</sub> > POSS-tetra-PEG<sub>20k</sub> > POSS-octa-PEG<sub>20k</sub>. POSS-tetra-PEG<sub>10k</sub> hydrogel was supposed to exhibit better adhesion properties.

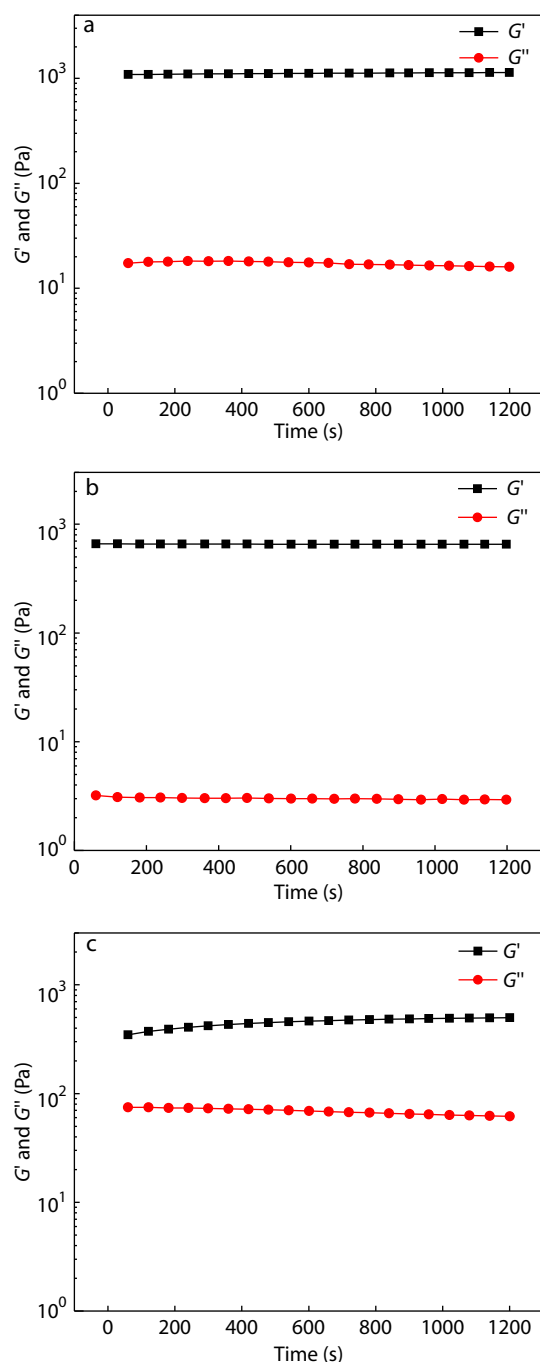


**Fig. 3**  $G'$  and  $G''$  of the hydrogels: (a) POSS-tetra-PEG<sub>10k</sub>, (b) POSS-tetra-PEG<sub>20k</sub> and (c) POSS-octa-PEG<sub>20k</sub>.

However, the longer gelation time of the POSS-tetra-PEG<sub>20k</sub> hydrogel may facilitate the succinimidyl ester groups to interact with the pigskin surface to exhibit superior adhesion strength. Hence, different gelation time caused by different types of PEG may be the main influencing factor on the adhesion property. And we chose POSS-tetra-PEG<sub>20k</sub> hydrogel as the experimental group for the subsequent exploration.

### Swelling and Degradation Properties of the POSS-ace-PEG Hydrogels

Since the acetal bonds could be broken into aldehydes and

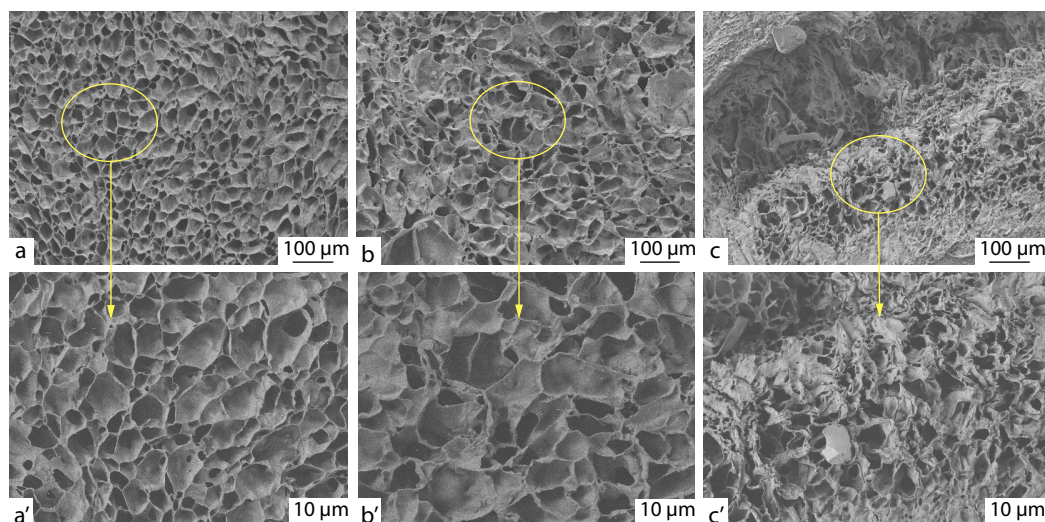


**Fig. 4** SEM images of the fractured surface of hydrogels: (a, a') POSS-tetra-PEG<sub>10k</sub>, (b, b') POSS-tetra-PEG<sub>20k</sub>, (c, c') POSS-octa-PEG<sub>20k</sub>. The images below are enlarged parts of the yellow-circle areas of the images above.

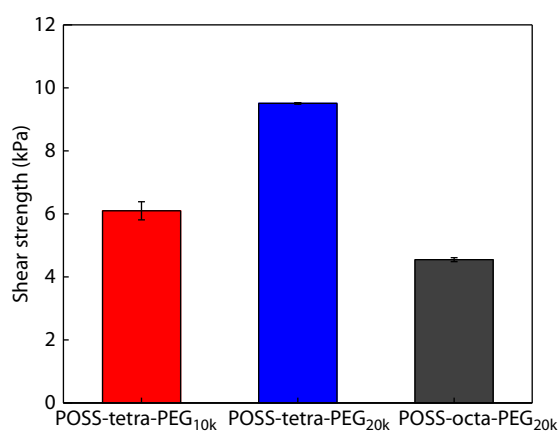


**Fig. 5** Shear strength of various POSS-ace-PEG hydrogels.

alcohol compounds under acidic conditions, the POSS-ace-PEG hydrogels showed acid-responsive degradation behavior. Firstly, we investigated the swelling performance of POSS-ace-PEG hydrogels under a physiological environment, and the pristine PEG hydrogels made of PEG-SC and PEG-NH<sub>2</sub> (4 arm, 20 kDa) with the same solid content were used as the control group. As shown in Fig. 6(a), the POSS-ace-PEG hydrogels exhibit similar swelling behavior as the pristine PEG hydrogels. This was partly because the PEG fraction as a hydrophilic backbone in the gel bore a large amount of water absorption, leading to a similar swelling ratio. On the other hand, although POSS-ace-PEG hydrogel contained the G1'-[NH<sub>2</sub>]<sub>16</sub> component with a certain degree of hydrophobicity, it had more defects compared to the pristine PEG hydrogel, causing an increase in the swelling ratio. Thus, the swelling ratio of POSS-ace-PEG hydrogels was overall similar to the pristine PEG hydrogels.

Furthermore, we verified the degradation property of POSS-ace-PEG hydrogels in pH 5.0 buffer. Fig. 6(b) shows that the POSS-ace-PEG hydrogels also has a rapid water absorption similar to pristine PEG hydrogels at the early stage of immersion. As time increased, the pristine PEG hydrogels con-

tinued to absorb water; while the shape of POSS-ace-PEG hydrogel gradually loosened in solution, leading to a significant decrease in the mass of the hydrogel. Finally, the hydrogel was disintegrated and dissolved completely in the buffer solution within 24–48 h. This was entirely attributed to the acetal structure of the G1'-[NH<sub>2</sub>]<sub>16</sub> component, which could achieve rapid degradation under acidic conditions, leading to the dissociation of the gel network.

#### Drug Release Profiles of DOX

Owing to the rapid degradation properties of POSS-ace-PEG hydrogels in acidic solutions, we further investigated the drug release properties of POSS-ace-PEG hydrogels in acidic media. We chose doxycycline hydrochloride (DOX) as a model drug to be loaded in the hydrogel because of its good hydrophilicity and uniform dispersion in the gel. On the other hand, DOX had a potential therapeutic effect on inflammatory environment around the tissue when the drug-loaded hydrogel was applied for tissue adhesion. As observed in Fig. 7, rapid drug release was achieved within 12 h in pH=7.4 buffer, but subsequently, a portion of the drug was retained in the hydrogel for a long time because the structure of POSS-ace-PEG hydrogel remained intact. However, along with the gradual degradation of POSS-ace-PEG hydrogel, inner drugs were easily escaped into the solutions under acidic environments, exhibiting a gradient increase in release rate. According to Fig. 6(b), after the hydrogel was soaked in pH=5.0 buffer for more than 12 h, its structure turned loose, separating into several dispersed blocks, and the mass dropped rapidly. Therefore, there was an accelerated release at this stage in drug delivery. Finally, the hydrogel was completely disintegrated in the buffer solution and the DOX were completely released for 48 h, which indicated that POSS-ace-PEG hydrogels had promising application prospects in acidic environments such as tumors and inflammation therapy.

#### Cytotoxicity Studies

A key objective of POSS-ace-PEG hydrogels as tissue adhesives is to maintain their functionality without damaging the biological activity of tissue cells. The main components of POSS-

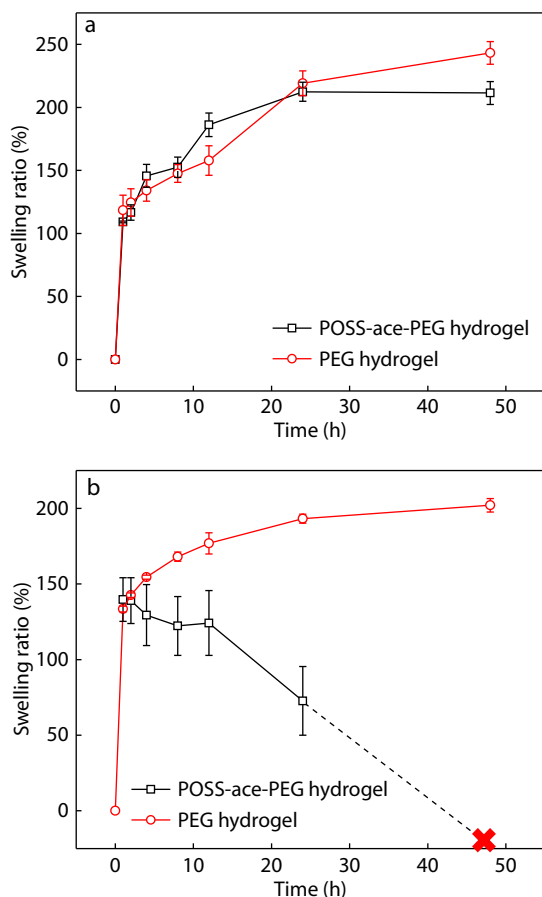


**Fig. 6** (a) Swelling at pH 7.4 and (b) degradation at pH 5.0 profiles of POSS-ace-PEG hydrogels.

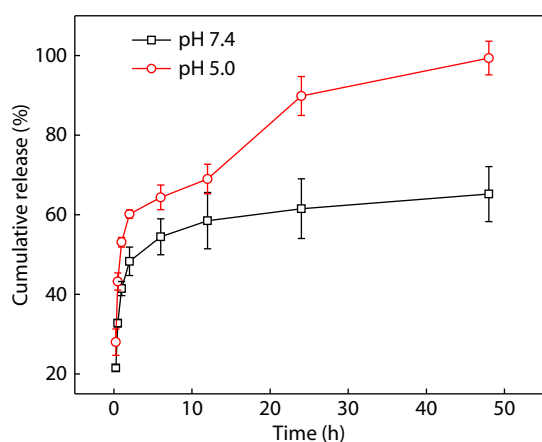


**Fig. 7** Release behaviors of DOX-loaded POSS-ace-PEG hydrogels at different pH conditions.

ace-PEG hydrogels were high molecular weight of PEG and dendritic polyacetal. PEG is a kind of recognized biocompatible macromolecule and has been widely used in a variety of FDA-approved medical products.<sup>[1]</sup> While the dendritic polyacetal has been proven to be used in biomedical materials in many studies due to the low toxicity of its degradation products.<sup>[35]</sup> To clearly illustrate the cytotoxicity of various POSS-ace-PEG hydrogels, we used 3T3 mouse fibroblasts as model cells. We

determined the cytotoxicity of both the extracts and degradation products of the POSS-ace-PEG hydrogels, which were formed from different types of PEG. The results show that the cell viability remained more than 85% in both the extract and degradation solutions after 1 and 3 days of incubation (Fig. 8), demonstrating that various POSS-ace-PEG hydrogels exhibited good cell safety and broad application prospects in tissue adhesives.

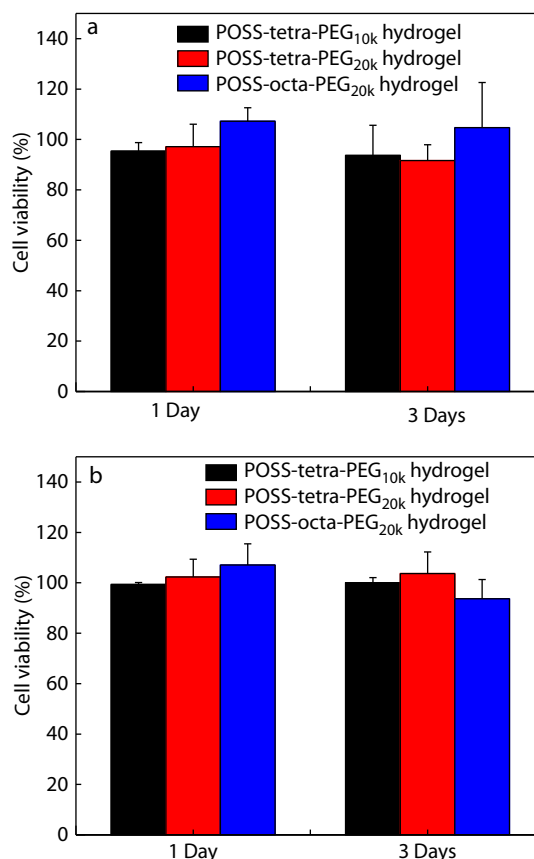


**Fig. 8** Cytotoxicity of (a) extract and (b) degradation solution of various POSS-ace-PEG hydrogels against NIH-3T3 fibroblasts after incubation for 1 and 3 days.

### **In Vitro Tissue Adhesive Properties of POSS-ace-PEG Hydrogels**

We explored the prospect of POSS-ace-PEG hydrogels as tissue adhesives by *in vitro* models. Firstly, we chose porcine skin as a model to demonstrate the adhesion of POSS-ace-PEG hydrogels. POSS-tetra-PEG<sub>20k</sub> hydrogel was formed *in situ* on the surface of porcine skin in which rhodamine B (red) was incorporated for better observation. Fig. 9(a) demonstrated that the hydrogel could also adhere to the pigskin without peeling off regardless of the pressure applied, such as twisting and bending. Combined with the results in Fig. 5, the POSS-ace-PEG hydrogel could achieve effective adhesion with skin tissues. For nerve tissues, adhesives can be a convenient adjunct to nerve repair.<sup>[5]</sup> We applied the POSS-ace-PEG hydrogel to the fractured nerve defect. As shown in Fig. 9(b), POSS-ace-PEG hydrogel could effectively bond the fractured nerve tissues together and remained stable in the suspended state, which

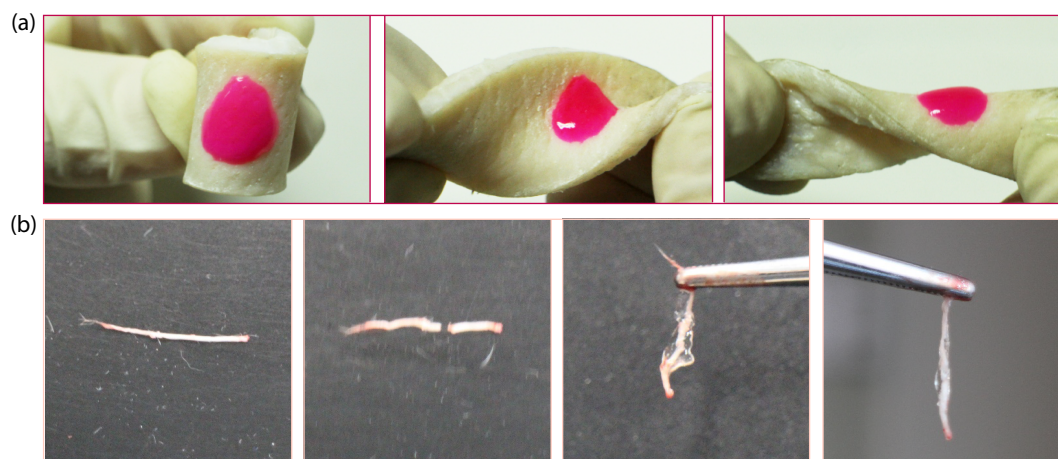


**Fig. 9** *In vitro* experiments results of POSS-ace-PEG hydrogel adhesion to (a) porcine skin and (b) fracture nerves.

might contribute to the field of neuro-restoration.

## CONCLUSIONS

In summary, we synthesized  $G1'-[NH_3Cl]_{16}$  with high-density amino groups on the periphery through Michael addition and "thiol-ene" reactions. Due to its regular structure and a controllable number of functional groups,  $G1'-[NH_3Cl]_{16}$  with high molecular weight and multi-armed PEG-SC were blended to prepare the POSS-ace-PEG hydrogels quickly. The obtained hydrogels exhibited porous structures, excellent mechanical strength and a high swelling ratio, which were necessary for tissue adhesion in critical situations. The presence of a large number of acetal bonds endowed the hydrogel with the property of intelligent degradation under acidic conditions, which in turn enabled the responsive release of antimicrobial drugs in an acidic environment, laying a solid foundation for its application prospects in acidic environments such as tumors and inflammation therapy. Cytological assays indicated that POSS-ace-PEG hydrogel system had good cell biocompatibility. The NHS-activated component enabled the hydrogels to have good adhesion to both porcine skin and neural tissues. The work demonstrated that this dendritic hydrogel system could be an ideal choice as a smart responsive platform for tissue adhesive.

## ACKNOWLEDGMENTS

This work was financially supported by the Ministry of Science and Technology of China (No. 2020YFA0908900), the National Natural Science Foundation of China (Nos. 21935011, 51973226, 21725403 and 81871782) and the Youth Innovation Promotion Association CAS (No. 2019031).

## REFERENCES

- Bouten, P. J. M.; Zonjee, M.; Bender, J.; Yauw, S. T. K.; van Goor, H.; van Hest, J. C. M.; Hoogenboom, R. The chemistry of tissue adhesive materials. *Prog. Polym. Sci.* **2014**, *39*, 1375–1405.
- Taboada, G. M.; Yang, K.; Pereira, M. J. N.; Liu, S. S.; Hu, Y.; Karp, J. M.; Artzi, N.; Lee, Y. Overcoming the translational barriers of tissue adhesives. *Nat. Rev. Mater.* **2020**, *5*, 310–329.
- Zhu, W. Z.; Chuah, Y. J.; Wang, D. A. Bioadhesives for internal medical applications: a review. *Acta Biomater.* **2018**, *74*, 1–16.
- Spotnitz, W. D.; Burks, S. Hemostats, sealants, and adhesives: components of the surgical toolbox. *Transfusion* **2008**, *48*, 1502–1516.
- Bu, Y.; Wang, X.; Li, L.; Hu, X.; Tan, D.; Li, Z.; Lai, M.; Qiu, X.; Sun, F.; Wang, H.; Yang, F.; Wu, D.; Guo, J. Lithium loaded octa-poly(ethylene glycol) based adhesive facilitates axon regeneration and reconnection of transected peripheral nerves. *Adv. Healthc. Mater.* **2020**, *9*, 2000268.
- Yang, J.; Bai, R.; Chen, B.; Suo, Z. Hydrogel adhesion: a supramolecular synergy of chemistry, topology, and mechanics. *Adv. Funct. Mater.* **2020**, *30*, 1901693.
- Thai Minh Duy, L.; Huu Thuy Trang, D.; Thambi, T.; Phan, V. H. G.; Jeong, J. H.; Lee, D. S. Bioinspired pH- and temperature-responsive injectable adhesive hydrogels with polyplexes promotes skin wound healing. *Biomacromolecules* **2018**, *19*, 3536–3548.
- Saghazadeh, S.; Rinoldi, C.; Schot, M.; Kashaf, S. S.; Sharifi, F.; Jalilian, E.; Nuutila, K.; Giatsidis, G.; Mostafalu, P.; Derakhshandeh, H.; Yue, K.; Swieszkowski, W.; Memic, A.; Tamayol, A.; Khademhosseini, A. Drug delivery systems and materials for wound healing applications. *Adv. Drug Deliv. Rev.* **2018**, *127*, 138–166.
- Liang, Y.; Zhao, X.; Ma, P. X.; Guo, B.; Du, Y.; Han, X. pH-Responsive injectable hydrogels with mucosal adhesiveness based on chitosan-grafted-dihydrocaffeic acid and oxidized pullulan for localized drug delivery. *J. Colloid Interface Sci.* **2019**, *536*, 224–234.
- Bu, Y.; Zhang, L.; Liu, J.; Zhang, L.; Li, T.; Shen, H.; Wang, X.; Yang, F.; Tang, P.; Wu, D. Synthesis and properties of hemostatic and bacteria-responsive *in situ* hydrogels for emergency treatment in critical situations. *ACS Appl. Mater. Interfaces* **2016**, *8*, 12674–12683.
- Liang, Y.; Zhao, X.; Hu, T.; Chen, B.; Yin, Z.; Ma, P. X.; Guo, B. Adhesive hemostatic conducting injectable composite hydrogels with sustained drug release and photothermal antibacterial activity to promote full-thickness skin regeneration during wound healing. *Small* **2019**, *15*, 1900046.
- Koetting, M. C.; Peters, J. T.; Steichen, S. D.; Peppas, N. A. Stimulus-responsive hydrogels: theory, modern advances, and applications. *Mater. Sci. Eng. R-Rep.* **2015**, *93*, 1–49.
- Annabi, N.; Tamayol, A.; Uquillas, J. A.; Akbari, M.; Bertassoni, L. E.; Cha, C.; Camci-Unal, G.; Dokmeci, M. R.; Peppas, N. A.; Khademhosseini, A. 25<sup>th</sup> Anniversary article: rational design and applications of hydrogels in regenerative medicine. *Adv. Mater.* **2014**, *26*, 85–124.
- Ferreira, N. N.; Ferreira, L. M. B.; Cardoso, V. M. O.; Boni, F. I.; Souza,

- A. L. R.; Gremiao, M. P. D. Recent advances in smart hydrogels for biomedical applications: from self-assembly to functional approaches. *Eur. Polym. J.* **2018**, *99*, 117–133.
- 15 Liao, J. X.; Huang, J. H.; Wang, T.; Sun, W. X.; Tong, Z. Rapid shape memory and pH-modulated spontaneous actuation of dopamine containing hydrogels. *Chinese J. Polym. Sci.* **2017**, *35*, 1297–1306.
- 16 Meng, F. D.; Ni, Y. X.; Ji, S. F.; Fu, X. H.; Wei, Y. H.; Sun, J.; Li, Z. B. Dual thermal- and pH-responsive polypeptide-based hydrogels. *Chinese J. Polym. Sci.* **2017**, *35*, 1243–1252.
- 17 Jiang, Z.; Tan, M. L.; Taheri, M.; Yan, Q.; Tsuzuki, T.; Gardiner, M. G.; Diggle, B.; Connal, L. A. Strong, self-healable, and recyclable visible-light-responsive hydrogel actuators. *Angew. Chem. Int. Ed.* **2020**, *59*, 7049–7056.
- 18 Kanamala, M.; Wilson, W. R.; Yang, M.; Palmer, B. D.; Wu, Z. Mechanisms and biomaterials in pH-responsive tumour targeted drug delivery: a review. *Biomaterials* **2016**, *85*, 152–167.
- 19 Wu, M.; Chen, J.; Huang, W.; Yan, B.; Peng, Q.; Liu, J.; Chen, L.; Zeng, H. Injectable and self-healing nanocomposite hydrogels with ultrasensitive pH-responsiveness and tunable mechanical properties: implications for controlled drug delivery. *Biomacromolecules* **2020**, *21*, 2409–2420.
- 20 He, J.; Shi, M.; Liang, Y.; Guo, B. Conductive adhesive self-healing nanocomposite hydrogel wound dressing for photothermal therapy of infected full-thickness skin wounds. *Chem. Eng. J.* **2020**, *394*, 124888.
- 21 Han, Z.; Wang, P.; Mao, G.; Yin, T.; Zhong, D.; Yiming, B.; Hu, X.; Jia, Z.; Nian, G.; Qu, S.; Yang, W. Dual pH-responsive hydrogel actuator for lipophilic drug delivery. *ACS Appl. Mater. Interfaces* **2020**, *12*, 12010–12017.
- 22 Lu, Y.; Aimetti, A. A.; Langer, R.; Gu, Z. Bioresponsive materials. *Nat. Rev. Mater.* **2017**, *2*, 16075.
- 23 Chai, Q.; Jiao, Y.; Yu, X. Hydrogels for biomedical applications: their characteristics and the mechanisms behind them. *Gels* **2017**, *3*, 6.
- 24 Raza, F.; Zhu, Y.; Chen, L.; You, X.; Zhang, J.; Khan, A.; Khan, M. W.; Hasnat, M.; Zafar, H.; Wu, J.; Ge, L. Paclitaxel-loaded pH responsive hydrogel based on self-assembled peptides for tumor targeting. *Biomater. Sci.* **2019**, *7*, 2023–2036.
- 25 Bazban-Shotorbani, S.; Hasani-Sadrabadi, M. M.; Karkhaneh, A.; Serpooshan, V.; Jacob, K. I.; Moshaverinia, A.; Mahmoudi, M. Revisiting structure-property relationship of pH-responsive polymers for drug delivery applications. *J. Control Release* **2017**, *253*, 46–63.
- 26 Schneider, L. A.; Korber, A.; Grabbe, S.; Dissemond, J. Influence of pH on wound-healing: a new perspective for wound-therapy? *Arch. Dermatol. Res.* **2007**, *298*, 413–420.
- 27 Dai, L.; Wang, Y.; Li, Z.; Wang, X.; Duan, C.; Zhao, W.; Xiong, C.; Nie, S.; Xu, Y.; Ni, Y. A multifunctional self-crosslinked chitosan/cationic guar gum composite hydrogel and its versatile uses in phosphate-containing water treatment and energy storage. *Carbohydr. Polym.* **2020**, *244*, 116472.
- 28 Pohlit, H.; Leibig, D.; Frey, H. Poly(ethylene glycol) dimethacrylates with cleavable ketal sites: precursors for cleavable PEG-hydrogels. *Macromol. Biosci.* **2017**, *17*, 1600532.
- 29 Liu, Y.; Li, Y.; Keskin, D.; Shi, L. Poly(beta-amino esters): synthesis, formulations, and their biomedical applications. *Adv. Funct. Mater.* **2019**, *8*, 1801359.
- 30 Li, Y.; Yang, L.; Zeng, Y.; Wu, Y.; Wei, Y.; Tao, L. Self-healing hydrogel with a double dynamic network comprising imine and borate ester linkages. *Chem. Mater.* **2019**, *31*, 5576–5583.
- 31 Gao, J.; Xu, Y.; Zheng, Y.; Wang, X.; Li, S.; Yan, G.; Wang, J.; Tang, R. pH-sensitive carboxymethyl chitosan hydrogels via acid-labile ortho ester linkage as an implantable drug delivery system. *Carbohydr. Polym.* **2019**, *225*, 115237.
- 32 Wang, W. L.; Ma, X. J.; Yu, X. F. pH-responsive polymersome based on PMCP-*b*-PDPA as a drug delivery system to enhance cellular internalization and intracellular drug release. *Chinese J. Polym. Sci.* **2017**, *35*, 1352–1362.
- 33 Zhang, J.; Jia, Y.; Li, X.; Hu, Y.; Li, X. Facile engineering of biocompatible materials with pH-modulated degradability. *Adv. Mater.* **2011**, *23*, 3035–3040.
- 34 Huang, D.; Zhuang, Y.; Shen, H.; Yang, F.; Wang, X.; Wu, D. Acetal-linked PEGylated paclitaxel prodrugs forming free-paclitaxel-loaded pH-responsive micelles with high drug loading capacity and improved drug delivery. *Mater. Sci. Eng. C* **2018**, *82*, 60–68.
- 35 Wang, Y.; Huang, D.; Wang, X.; Yang, F.; Shen, H.; Wu, D. Fabrication of zwitterionic and pH-responsive polyacetal dendrimers for anticancer drug delivery. *Biomater. Sci.* **2019**, *7*, 3238–3248.
- 36 Huang, D.; Wang, Y.; Yang, F.; Shen, H.; Weng, Z.; Wu, D. Charge-reversible and pH-responsive biodegradable micelles and vesicles from linear-dendritic supramolecular amphiphiles for anticancer drug delivery. *Polym. Chem.* **2017**, *8*, 6675–6687.
- 37 Huang, D.; Yang, F.; Wang, X.; Shen, H.; You, Y.; Wu, D. Facile synthesis and self-assembly behaviour of pH-responsive degradable polyacetal dendrimers. *Polym. Chem.* **2016**, *7*, 6154–6158.
- 38 Chen, P. Y.; Li, Z. The design of second-order nonlinear optical dendrimers: from "branch only" to "root containing". *Chinese J. Polym. Sci.* **2017**, *35*, 793–798.
- 39 Kim, Y.; Park, E. J.; Na, D. H. Recent progress in dendrimer-based nanomedicine development. *Arch. Pharm. Res.* **2018**, *41*, 571–582.
- 40 Fu, F. F.; Zhou, B. Q.; Ouyang, Z. J.; Wu, Y. L.; Zhu, J. Y.; Shen, M. W.; Xia, J. D.; Shi, X. Y. Multifunctional cholesterol-modified dendrimers for targeted drug delivery to cancer cells expressing folate receptors. *Chinese J. Polym. Sci.* **2019**, *37*, 129–135.
- 41 Kesharwani, P.; Lyer, A. K. Recent advances in dendrimer-based nanovectors for tumor-targeted drug and gene delivery. *Drug Discov. Today* **2015**, *20*, 536–547.
- 42 Mignani, S.; Rodrigues, J.; Tomas, H.; Zablocka, M.; Shi, X.; Caminade, A. M.; Majoral, J. P. Dendrimers in combination with natural products and analogues as anti-cancer agents. *Chem. Soc. Rev.* **2018**, *47*, 514–532.
- 43 Ghobril, C.; Grinstaff, M. W. The chemistry and engineering of polymeric hydrogel adhesives for wound closure: a tutorial. *Chem. Soc. Rev.* **2015**, *44*, 1820–1835.
- 44 Ghobril, C.; Charoen, K.; Rodriguez, E. K.; Nazarian, A.; Grinstaff, M. W. A dendritic thioester hydrogel based on thiol-thioester exchange as a dissolvable sealant system for wound closure. *Angew. Chem. Int. Ed.* **2013**, *52*, 14070–14074.
- 45 Wang, X.; Yang, Y.; Gao, P.; Li, D.; Yang, F.; Shen, H.; Guo, H.; Xu, F.; Wu, D. POSS dendrimers constructed from a 1→7 branching monomer. *Chem. Commun.* **2014**, *50*, 6126–6129.
- 46 Yuk, H.; Zhang, T.; Lin, S.; Parada, G. A.; Zhao, X. Tough bonding of hydrogels to diverse non-porous surfaces. *Nat. Mater.* **2016**, *15*, 190–196.
- 47 Shi, H.; Yang, J.; You, M.; Li, Z.; He, C. Polyhedral oligomeric silsesquioxanes (POSS)-based hybrid soft gels: molecular design, material advantages, and emerging applications. *ACS Mater. Lett.* **2020**, *2*, 296–316.
- 48 Li, Z.; Kong, J.; Wang, F.; He, C. Polyhedral oligomeric silsesquioxanes (POSSs): an important building block for organic optoelectronic materials. *J. Mater. Chem. C* **2017**, *5*, 5283–5298.
- 49 Fan, X.; Cao, M.; Zhang, X.; Li, Z. Synthesis of star-like hybrid POSS-(PDMAEMA-*b*-PDLA) 8 copolymer and its stereocomplex properties with PLLA. *Mater. Sci. Eng. C* **2017**, *76*, 211–216.
- 50 Li, Z.; Tan, B.; Jin, G.; Li, K.; He, C. Design of polyhedral oligomeric silsesquioxane (POSS) based thermo-responsive amphiphilic hybrid copolymers for thermally denatured protein protection applications. *Polym. Chem.* **2014**, *5*, 6740–6753.
- 51 Song, X.; Zhang, X.; Li, T.; Li, Z.; Chi, H. Mechanically robust hybrid POSS thermoplastic polyurethanes with enhanced surface hydrophobicity. *Polymers* **2019**, *11*, 373.
- 52 Rebrov, E. A.; Leshchiner, I. D.; Muzafarov, A. M. Synthesis of carbosilane dendrimers with variable distance between branching nodes. *Macromolecules* **2012**, *45*, 8796–8804.